PEEK Oligomers: A Model for the Polymer Physical Behavior. 1. Synthesis and Characterization of Linear Monodisperse Oligomers

Alain Jonas,*,[1] Roger Legras, and Jacques Devaux

Laboratoire de Physique et de Chimie des Hauts Polymères, Université Catholique de Louvain, Place Croix du Sud, 1, B-1348 Louvain-la-Neuve, Belgium

Received March 30, 1992; Revised Manuscript Received July 8, 1992

ABSTRACT: PEEK linear monodisperse oligomers have been synthesized by an iterative two-step route. Nucleophilic substitution of the fluorine end groups of a fluoroaryl ketone-ended *n*-mer by *p*-phenoxyphenol in the presence of sodium carbonate yielded a phenoxy-ended *n*-mer. Then a Friedel–Crafts acylation of the terminal phenyls of this compound was performed using 4-fluorobenzoic acid as the acylating agent in the superacid solvent CF_3SO_3H to obtain a fluoroaryl ketone-ended (*n* + 2)-mer. A simple kinetic analysis of the electrophilic reaction is performed with the aid of ^{19}F NMR. A side reaction was detected for strong reagent dilution. Various spectroscopic results indicate that this side reaction is due to the presence in solution of protonated ketones, which act as electrophiles competing with the acylating agent. The results of the kinetic analysis support a mechanism in which the acylium cation (or a protonated mixed anhydride) is the acylating agent. Spectroscopic characterization of the oligomers confirms the expected structures.

Introduction

Poly(oxy-1,4-phenyleneoxy-1,4-phenylenecarbonyl-1,4-phenylene) (PEEK) is a semicrystalline aromatic thermoplastic polymer whose remarkable engineering properties have stimulated much research. However, numerous terrae incognitae subsist in the knowledge of this polymer. This is true of the structural characterization of PEEK (crystal structure, semicrystalline morphology, etc.) as well as of its chemical behavior, especially at the high temperatures at which it is processed.

The PEEK crystal structure has been determined by various authors;[2–6] the ether and ketone bridges are crystallographically equivalent.[7] However, recent theoretical results from Abraham and Haworth[8] predict that various crystalline chain packings exist which differ in the relative placement of the ketone and ether bridges in the orthorhombic crystal unit cell. The large variation of the crystal unit cell density with crystallization temperature[9,10] (T_c) has been interpreted as being due to a transition from a disordered to an ordered bridge relative placement, although no experimental observation of such an ordering has been reported yet.

The PEEK thermodynamic melting temperature ($T_m°$) is reportedly in the range 389–395 °C;[11,12] it was determined with the aid of lamellar structure–melting relationships. However, these experiments were performed on bulk-crystallized polymers, whose structure is still relatively badly characterized. Indeed it was shown by specific heat measurements[13,14] that considerable amounts of a so-called rigid amorphous fraction exist in bulk-crystallized PEEK. This raises some doubt about the validity of a simple two-phase model to represent the physical structure of bulk-crystallized PEEK and, thus, about the adequacy of the lamellar structure–melting relationships used to determine $T_m°$.

Polymer single crystals are very helpful in determining the crystal structure and properties of a polymer. However, the lack of solubility of PEEK precludes growing perfect single crystals; PEEK single crystals reported in the literature[15–18] are invariably very disordered. The use of monodisperse oligomers of PEEK may overcome this problem. Indeed, crystals of such oligomers may have more regular structures than PEEK crystals and be easier to structurally characterize. Polymer properties could then be obtained by extrapolation to longer chain lengths.

Such oligomers would also be ideal model compounds to study the thermal degradation of the parent polymer. For instance, any molecular mass perturbations resulting from a given processing condition would be easy to detect on monodiperse oligomers. Moreover, chain end effects can be determined, which is particularly interesting since chain ends influence polymer thermal stability[14] and, when ionic, nucleate polymer crystals.[19]

In this series of papers, we report the synthesis and structural characterization of linear PEEK monodisperse oligomers with molecular masses from 507 to 1371. This paper presents the oligomer synthesis and spectroscopic analysis. The second paper of this series will present the structure and thermal behavior of the oligomer crystals.[20] In the third paper of this series,[21] the properties of some oligomers extracted from the commercial polymer will be examined and compared with the monodisperse linear oligomers.

Results and Discussion

General Synthesis Scheme and Nomenclature. The oligomers were synthesized by an iterative two-step route. The fluorine end groups of a fluoroaryl ketone-ended *n*-mer (1), abbreviated as $FK(EEK)_nF$, were substituted by *p*-phenoxyphenol (2) in the presence of sodium carbonate using reaction conditions analogous to the usual PEEK synthesis.[22]

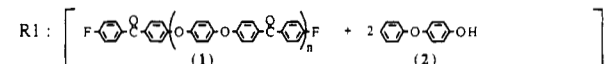

The reaction produces the phenoxy-ended *n*-mer (3) in high yields, abbreviated as $EEK(EEK)_nEE$. Then a Friedel–Crafts acylation of the terminal phenyls of 3 was performed with 4-fluorobenzoic acid (4) as the acylating agent; trifluoromethanesulfonic (triflic) acid (CF_3SO_3H) was used as both the solvent and catalyst.

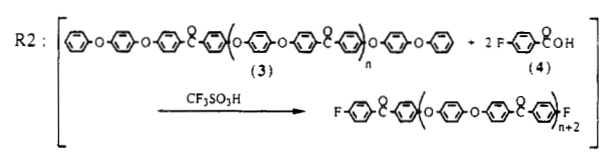

The fluoroaryl ketone-ended (*n* + 2)-mer was obtained. This type of electrophilic reaction was studied by Roberts

0024-9297/92/2225-5841$03.00/0

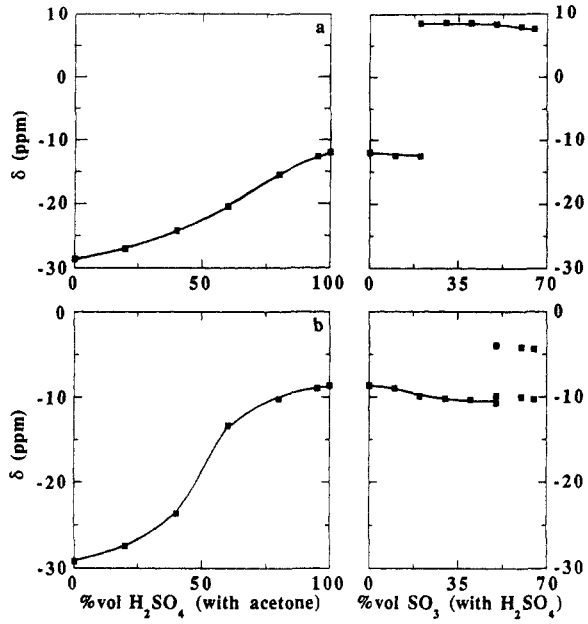

Figure 1. Evolution with solvent acid strength (H_2SO_4 solutions) of ^{19}F NMR chemical shifts of 4-fluorobenzoic acid (a) and 4,4′-difluorobenzophenone (b).

and Sadri[23] and used later by Colquhoun and Lewis[24] to synthesize PEEK. Starting from 4,4′-difluorobenzophenone ($FK(EEK)_0F$) and 4,4′-diphenoxybenzene (EE), the whole series of linear oligomers can theoretically be obtained. However, only the n = 0–2 phenoxy-ended oligomers (3) and the n = 1–4 fluoroaryl ketone-ended oligomers (1) will be presented here. Longer oligomers were not synthesized, since the structural information obtained from the shortest oligomers study[20] was sufficient for our purposes.

Although the nucleophilic substitution is a well-understood and reliable reaction, it was necessary to examine the kinetics of the electrophilic substitution. Indeed, a side reaction was sometimes detected, and the conversion was limited using certain synthesis conditions.

Acylation Kinetics. Protonation Studies. To determine the extent of protonation of the reagents and products of R2 in the strongly acidic synthetic conditions, ^{19}F NMR studies were first conducted in sulfuric acid solutions of increasing acidities. The method was inspired by a previous study[25] that monitored the protonation of various carboxylic acids by ^1H NMR spectroscopy. As shown in Figure 1, the ^{19}F resonance of 4 shifts downfield with increasing acid strength until a plateau is reached at 100% H_2SO_4. The downfield shift reflects the progressive protonation of 4 (R3), leading to the protonated acid (5). Only one resonance is observed at these acid strengths due to fast exchange between 4 and 5. However, after addition of 20 vol % SO_3, a doubling of peaks appears. This behavior is due to formation of the acylium cation (6) from the protonated acid (R4).

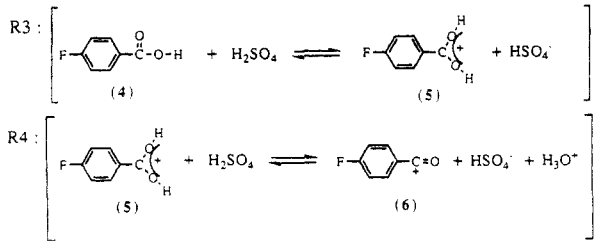

The formation of the acylium cation in superacid solutions is well documented.[26-28] The 21.1 ppm ^{19}F chemical shift difference between the two forms 5 and 6 agrees well with that published by Olah et al. (20.21 ppm in FSO_3H–SbF_5).[26] The slight decrease of the chemical shift upon further acid strength increase is probably due to protonation of the shift reference. Since two peaks are observed at 20% SO_3, a slow exchange rate between 5 and 6 exists. This is not surprising, since the back-conversion of 6 into 5 requires the cooperation of three ionic species. Following Gillespie and Peel,[29] the H_0 value of the 20 vol % SO_3 oleum is of the order of −13.5. The H_0 value of triflic acid has been reported to be −14.1[30] and −13.[31] It is thus not clear if the acylium ion is produced in significant amounts in triflic acid. This point will be studied later.

The chemical shift of 4,4′-difluorobenzophenone (7), a model compound for the ketones of the reaction products, increases very rapidly with increasing acid strength since ketones are basic (Figure 1). 4,4′-Difluorobenzophenone is already completely protonated in 95% sulfuric acid. Upon further increase in acid strength, the chemical shift remains constant; the slight decrease observed is again attributed to variations in the chemical shift of the reference. Above 50 vol % SO_3, multiple resonance peaks are observed, probably due to the sulfonation of one of the aromatic rings, making the two fluorine atoms of 7 chemically inequivalent.

Additional experiments were conducted in triflic acid to better simulate the synthetic conditions. This acid has the advantage that it is not a sulfonating agent. Small amounts of 4 or $FK(EEK)_2F$ were added to triflic acid, scanning the majority of experimental concentrations used for kinetic studies. CF_3SO_3Na was also added to simulate the existence in the reaction medium of $CF_3SO_3^-$ anions produced by the protonation of other reagents or products and by the reaction itself.

The $FK(EEK)_2F$ chemical shifts were constant for $FK(EEK)_2F$ concentrations of 0.012–0.25 mol L^{-1} and CF_3SO_3Na concentrations from 0 to 0.4 mol L^{-1}. The maximum shift variation of 0.05 ppm is clearly negligible. In accordance with the above observation that 7 is fully protonated in 95% sulfuric acid (H_0 = −9.8[29]), we conclude that $FK(EEK)_2F$ is fully protonated in the concentration range corresponding to our reaction conditions.

Following the initial concentrations of 4 (0.04–3.6 mol L^{-1}) and of CF_3SO_3Na (0–0.41 mol L^{-1}), the chemical shift of 4 varied betweem −11.31 and −14.29 ppm. These variations are due to the equilibrium between the various forms 4, 8, and 9 (R5 and R6).

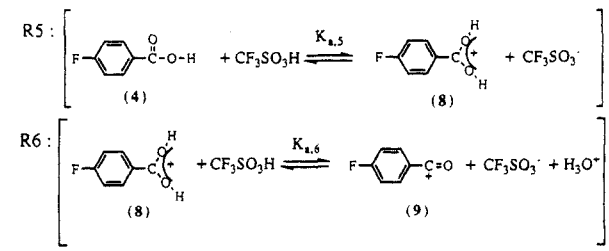

As an alternative to R6, formation of a protonated mixed anhydride (10) has also been proposed by Roberts and Sadri[23] (R7).

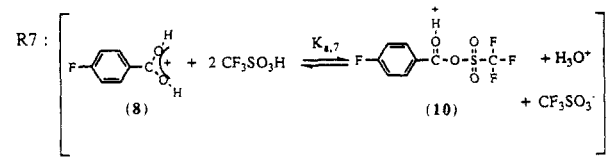

The term FBA will hereafter designate this equilibrium

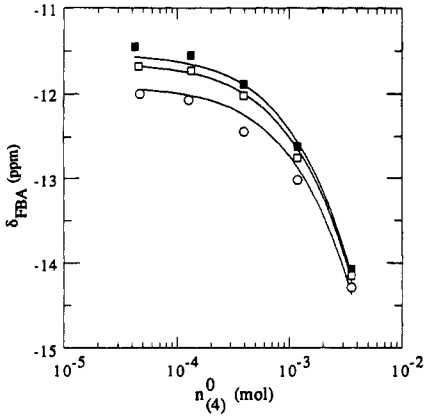

Figure 2. Evolution of ^{19}F NMR chemical shift of 4-fluorobenzoic acid (FBA) upon progressive dilution in 1 mL of CF_3SO_3H with 0 (■), 1.15×10^{-4} (□), and 4.1×10^{-4} mol (○) of added CF_3SO_3Na. The lines are fit theoretical relationships.

of **4**, **8**, and **9** or **10**. With $n^\circ_{(TfOH)}$, $n^\circ_{(4)}$, and $n^\circ_{(TfO^-)}$ the initial mole numbers of CF_3SO_3H, **4**, and CF_3SO_3Na, respectively, the (R5) equilibrium constant can be written as

$$K_{a,5} = K_{\gamma,5}\frac{(n^\circ_{(TfO^-)} + n_{(8)} + 2n_{(9)})n_{(8)}}{(n^\circ_{(TfOH)} - n_{(8)} - 2n_{(9)})(n^\circ_{(4)} - n_{(8)} - n_{(9)})} \quad (1)$$

with $n_{(8)}$ the equilibrium mole number of **8** and $n_{(9)}$ the equilibrium mole number of **9**. $K_{\gamma,5}$ contains terms due to activity coefficients. This equation applies only if the (R6) equilibrium is considered to be the relevant one. If equilibrium (R7) is used instead of (R6), then eq 1 must be slightly transformed into

$$K_{a,5} = K_{\gamma,5}\frac{(n^\circ_{(TfO^-)} + n_{(8)} + 2n_{(10)})n_{(8)}}{(n^\circ_{(TfOH)} - n_{(8)} - 3n_{(10)})(n^\circ_{(4)} - n_{(8)} - n_{(10)})} \quad (2)$$

with $n_{(10)}$ the equilibrium mole number of **10**.

The measured ^{19}F NMR chemical shift of FBA, δ_{FBA}, is always very close to the chemical shift of **5** (similar to **8**) and very far away from the chemical shift of **6** (similar to **9**). We thus assume that $n_{(9)} \ll n_{(8)}$ (or $n_{(10)} \ll n_{(8)}$). Hence, eqs 1 and 2 both reduce to eq 3.

$$K_{a,5} = K_{\gamma,5}\frac{(n^\circ_{(TfO^-)} + n_{(8)})n_{(8)}}{(n^\circ_{(TfOH)} - n_{(8)})(n^\circ_{(4)} - n_{(8)})} \quad (3)$$

Based on the same hypothesis, δ_{FBA} is in the fast exchange rate condition:[32]

$$\delta_{FBA} = \frac{n_{(8)}}{n^\circ_{(4)}}\delta_8 + \frac{n^\circ_{(4)} - n_{(8)}}{n^\circ_{(4)}}\delta_4 \quad (4)$$

with δ_4 and δ_8 the chemical shifts of **4** and **8** relative to the solvent peak.

The experimental results were fit to eqs 3 and 4, assuming that $K_{\gamma,5}$ is constant. The fit parameters were found to be $K_{a,5}/K_{\gamma,5} = 1.04$, $\delta_4 = -22.60$ ppm, and $\delta_8 = -11.53$ ppm. Experimental NMR shifts, along with computed values, are plotted in Figure 2 versus $n^\circ_{(4)}$ for various $n^\circ_{(TfO^-)}$. The computed values are close to the experimental points. The chemical shift of **8** (δ_8) is similar to that of **5** (≃**8**) (−11.99 ppm), the difference probably being due to solvent effects and to the approximations made. The agreement between δ_4 and the chemical shift of **4** measured in acetone (−28.6 ppm) is less satisfactory, but the nature of the solvents is much different; moreover, since the measured chemical shifts are always higher than −15 ppm, one expects for numerical reasons a much larger error in δ_4 than in δ_8.

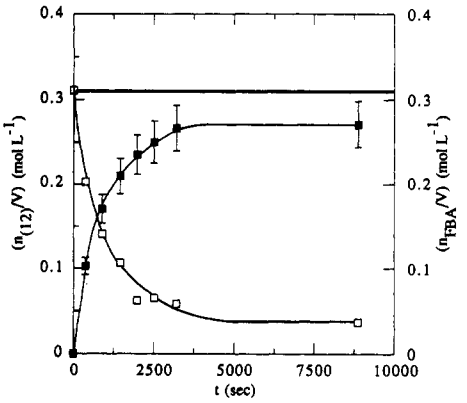

Figure 3. Typical kinetic curve obtained by ^{19}F NMR (sample 5 of Table I): (■) concentration of fluoroaryl ketone chain ends ($n_{(12)}/V$) vs time t; (□) concentration of 4-fluorobenzoic acid (n_{FBA}/V) vs time t. The horizontal line represents the amount of fluoroarylketone chain ends expected from stoichiometric considerations.

Since δ_{FBA} spans identical ranges in the kinetics experiments and in the present protonation study, it is valid to use the parameters calculated from the protonation study to compute $n_{(8)}$ in the kinetics experiments by using eq 4. This will provide values for the extent of protonation of unreacted **4** throughout the course of the reaction.

Kinetics Studies. The acylation kinetics of the EEKEE oligomer (**11**) by **4** has been followed at room temperature with the aid of ^{19}F NMR, changing the initial ratios of **4** to **11** from 2.2:1 to 10:1 and the molar ratio of CF_3SO_3H to **11** from 25:1 to 350:1. A typical evolution of the amount of FBA ($n_{(FBA)}$) and of fluoroaryl ketone chain ends created during the synthesis (**12**) ($n_{(12)}$) is presented in Figure 3 versus reaction time t.

The reaction pseudo-half-life $\tau_{1/2}$ and the final yield η calculated from the ratio of the amount of fluoroaryl ketone chain ends obtained and the amount expected from stoichiometry are summarized in Table I. This table also includes results of the acylation of $EEK(EEK)_2EE$. The rate constant is similar to the EEKEE acylation constant. Figure 4 plots η and $\tau_{1/2}$ as a function of the initial molar ratio of CF_3SO_3H to **11** using a 10% excess of **4**.

An increase in $\tau_{1/2}$ with increasing concentration was also observed by Colquhoun and Lewis.[24] The decrease of η with dilution is not due to a decrease in the NMR sensitivity with dilution but indicates that there is a competing side reaction that prevents complete acylation. Indeed, the standard deviation of ^{19}F NMR peak areas measured using solutions of known concentrations is 2–7% depending on concentration. Overall, the measured values are within ~10% of their actual value, which is lower than the variations measured for η. This implies that another reaction is consuming phenoxy chain ends in parallel competition with the acylation.

The NMR results fit the following second-order kinetic equation:

$$\frac{dn_{(12)}}{dt} = \frac{k}{V}(n^\circ_{(4)} - n_{(12)})(2n^\circ_{(11)} - n_{(12)}) \quad (5)$$

in which V is the solution volume (2 mL), $n_{(12)}$ is the number of fluoroaryl ketone chain ends created at time t, and $n^\circ_{(4)}$ and $n^\circ_{(11)}$ are the initial amounts of fluorobenzoic acid (**4**) and EEKEE (**11**), respectively. Assuming that the side reaction does not affect the overall kinetics, eq 5 expresses that the two successive acylations are described by two second-order equations having the same rate constant k (R8–R9). Each acylation is therefore independent of the nature of the other chain end.

Table I
Kinetic Analysis Results of EEKEE and EEK(EEK)$_2$EE Acylation by 4

sample	[CF_3SO_3H]/[EEKEE]	[FC_6H_4COOH]/[EEKEE]	$\tau_{1/2}$ (s)	η ($\pm\sigma^a$) (%)	$k \times 10^{-3}$ (L mol^{-1} s^{-1})	$n_{(8)}/n_{(FBA)}$ (%)
1	350	2.2	<200	42 (±3.5)	>16[b,c]	97.3
2	350	8		56 (—)		
3	200	2.2	<300	68 (±3)	>39[b,c]	97.1–97.3
4	200	10	<225	78 (±4.7)	>11[b,c]	92.2–92.3
5	71	2.2	730	87 (±3)	5.6	90.3–91.0
6	71	2.2[d]	650	87 (±2)	3.4	86.9–87.8
7	71	4	640	84 (—)	2.5	86.6–87.1
8	71	8	~350	100 (±6)	~2.4[c]	82.6–83.4
9	25	2.2	2400		0.45	80.1–80.7
10	25	4	>60000		0.011	69.3–71.2

[a] σ is the measured standard deviation of η. [b] Only an order of magnitude of k is given, due to significant competition of side reactions with the acylation. [c] Only a lower bound to k is given, due to a too fast reaction rate as compared to the NMR accumulation time. [d] EEK(EEK)$_2$EE acylation.

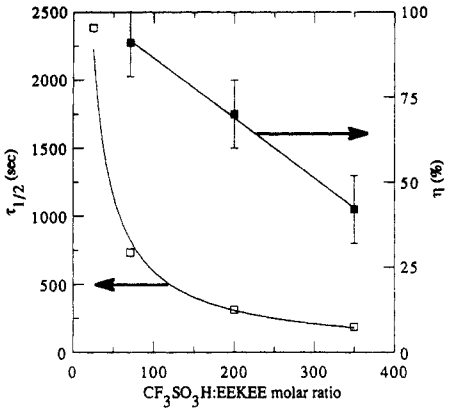

Figure 4. Evolution of the acylation pseudo-half-life $\tau_{1/2}$ (□) and final yield η (■) with reagent (EEKEE) dilution in triflic acid (10% excess of 4-fluorobenzoic acid).

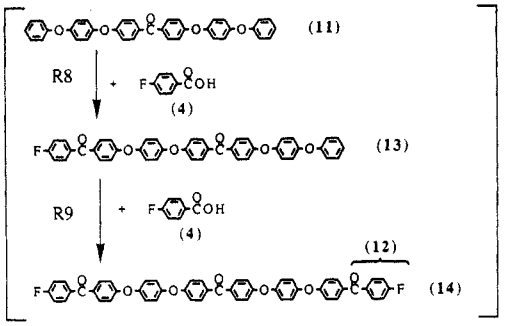

Consequently

$$\frac{dn_{(FBA)}}{dt} = -\frac{k}{V} n_{(FBA)}(2n_{(11)} + n_{(13)}) \qquad (6)$$

in which $n_{(13)}$ is the number of moles of 13 at time t and the factor 2 is due to the fact that the probability of 4 reacting with 11 is twice the probability of it reacting with 13. Since

$$n^\circ_{(11)} = n_{(11)} + n_{(13)} + n_{(14)} \qquad (7)$$

and

$$n^\circ_{(4)} = n_{(FBA)} + n_{(13)} + 2n_{(14)} \qquad (8)$$

eq 6 becomes

$$\frac{dn_{(FBA)}}{dt} = -\frac{k}{V} n_{(FBA)}(n_{(FBA)} + 2n^\circ_{(11)} - n^\circ_{(4)}) \qquad (9)$$

Using the following expression for the number of fluoroaryl ketone chain ends (12) in solution

$$n_{(12)} = n^\circ_{(4)} - n_{(FBA)} \qquad (10)$$

eq 5 is obtained by combining eqs 9 and 10.

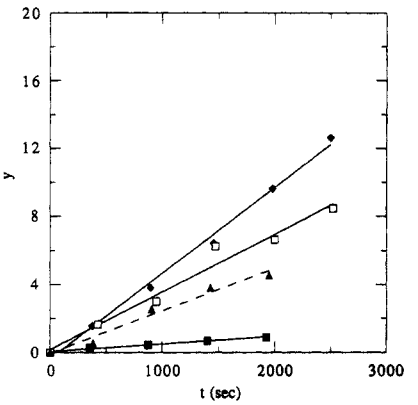

Figure 5. Representative fits of the second-order equation (eq 5) to the experimental kinetic results. The ordinate y is defined in the text. The following samples are presented (refer to Table I): (♦, 5); (□, 6); (▲, 7); (■, 9).

Resolution of eq 5 leads to a linear relationship of slope k between reaction time and y, where y has the following meaning:

$$y = \frac{V}{n^\circ_{(4)} - 2n^\circ_{(11)}}\left(\ln\frac{n^\circ_{(4)} - n_{(12)}}{2n^\circ_{(11)} - n_{(12)}} - \ln\frac{n^\circ_{(4)}}{2n^\circ_{(11)}}\right) \quad \text{when } n^\circ_{(4)} \gg 2n^\circ_{(11)}$$

$$y = \frac{V}{n^\circ_{(4)} - n_{(12)}} - \frac{V}{n^\circ_{(4)}} - \frac{V(2n^\circ_{(11)} - n^\circ_{(4)})}{2}((n^\circ_{(4)} - n_{(12)})^{-2} - (n^\circ_{(4)})^{-2}) \quad \text{when } 2n^\circ_{(11)} \cong n^\circ_{(4)}$$

Representative fits of the experimental results to the integral form of eq 5 are shown in Figure 5. The use of eq 5 is clearly not justified when η is lower than ~85%, i.e., when the side reaction is significant compared to the precision of the measurements (~10%). Hence, the fitting was performed only for experiments having η above ~85%.

The fits are satisfactory within experimental errors. The results are presented in Table I. The values k/V and $\tau_{1/2}^{-1}$ decrease with increasing concentration. In some cases, the kinetics are too rapid to obtain more than two or three points before the reaction is completed. For these samples, only a lower bound to k/V could be computed. For the highest dilutions, the side reaction is important and only the order of magnitude of k/V was estimated.

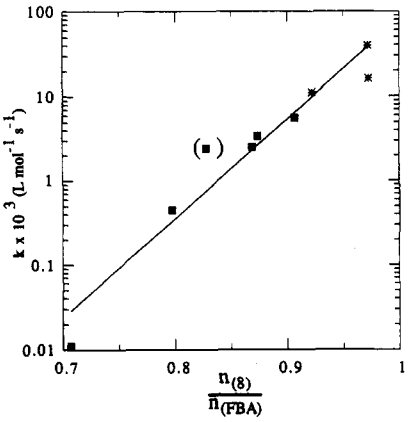

Figure 6. Evolution of the second-order rate constant k (eq 5) with acid strength of the reaction medium ($n_{(8)}/n_{(FBA)}$). (*) Conditions for which the side reaction is significantly detected. The point in parentheses is related to a reaction whose course was too rapid to perform a reliable analysis.

To understand the evolution of k with dilution, the amount of protonated fluorobenzoic acid (8) relative to the total amount of FBA at time t in the reacting solution ($n_{(8)}/n_{(FBA)} = n_{(8)}/(n_{(4)} + n_{(8)})$) was computed from the measured ^{19}F NMR shift of FBA at time t, using the chemical shifts of pure 8 and 4 determined previously and eq 4 in which $n^{\circ}_{(4)}$ is replaced by $n_{(FBA)}$. Since the ^{19}F NMR shifts of FBA are almost constant during the reaction, the $n_{(8)}/n_{(FBA)}$ ratio is also constant for each experiment within 2.5% and in most cases within 1%.[33] However, $n_{(8)}/n_{(FBA)}$ varies strongly from experiment to experiment due to the different amounts of $CF_3SO_3^-$ produced by protonation of the reagents and products. This ratio is a function of the acid strength of the reaction medium, since the higher the acid strength, the higher the amount of protonated fluorobenzoic acid. The $n_{(8)}/n_{(FBA)}$ ratios are summarized in Table I. A plot of k versus this ratio is presented in Figure 6.

There is an exponential correlation between k and $n_{(8)}/n_{(FBA)}$. This is due to the (R6) (or (R7)) equilibrium, which is shifted toward the reverse direction with decreasing acidity (increasing $CF_3SO_3^-$ concentration). Upon concentration of the reagents, the higher concentration of $CF_3SO_3^-$ anions produced by protonation and by the acylation disfavors formation of the actual electrophilic species, 9 or 10, from the protonated acid 8. There are fewer electrophilic species produced relative to the amount of 4 introduced. The reaction rate is thus not simply proportional to the concentration of 4 in solution; the rate constant decreases with increasing concentration of 4. This however is not equivalent to saying that the reaction rate decreases, since this rate formally depends on the product of the rate constant and the concentrations of FBA and 11. The displacement of the (R6) equilibrium to the left with increasing $CF_3SO_3^-$ explains why the reaction pseudo-half-life decreases with increasing dilution (Figure 4).

Side Reactions. In this section, experimental results related to side reactions are presented. There are in the reacting medium other electrophiles which may compete with the acylium cation. Protonated ketones are such electrophiles. Furthermore, there are various nucleophilic sites whereon the electrophilic attack may occur. Carbon atoms located on the diether-flanked rings and orthocarbons of the terminal monosubstituted phenyl rings are potential sites for electrophilic reactions. Consequently, η is significantly lower than 100% for some reacting conditions.

(a) Nucleophilic Sites. It is known that aromatic compounds containing ortho,para-directing groups like phenoxy groups are easily acylated and give mainly or exclusively the para products, because of the relatively large size of the acyl group.[34] Thus, large amounts of ortho substitution are not to be expected. This is indeed confirmed by the fact that no additional ^{19}F resonance peak could ever be observed during the acylation reactions. The same observation holds for the possible acylation of diether-flanked rings. Steric reasons probably favor the selective para acylation of the terminal phenyls.

(b) Electrophiles. The condensation of aromatic rings with protonated ketones, or hydroxyalkylation, is a well-known reaction which has been used for the production of phenol–formaldehyde type resins.[34] There are two types of protonated ketones in our reacting medium, namely, fluoroaryl ketone protonated chain ends and protonated interior ketones. The first ones should be more electrophilic due to the fluorine presence, which decreases the cation stability. Each electrophile could a priori attack any of the three nucleophilic sites. However, it is unlikely that the diether-flanked rings or the ortho carbons of the terminal phenyls could be substituted by such bulky electrophiles. On the contrary, the substitution of the para carbon of the terminal phenyls by these electrophiles should be considered.

(b1) Autocondensation of 11. To obtain information on the potential para substitution of terminal phenyls by protonated interior ketones, we have studied the evolution of 11 when dissolved alone in triflic acid. In this case, there is only one electrophile in the reacting medium, namely, the protonated interior ketone. The electrophilic attack of the terminal phenyl by the protonated ketone may lead first to a substituted triphenylmethanol (15) following (R10), which in strong acids is readily converted (R11) into a very stable substituted triphenylmethyl cation (16).[26]

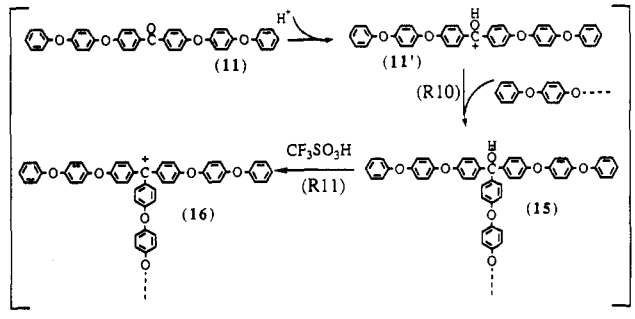

The ^{13}C NMR spectra of 11 taken in *N*-methyl-2-pyrrolidone at 100 °C before and after treatment with triflic acid for 48 h ($n_{(CF_3SO_3H)}:n_{(11)}$ = 250:1) are shown in Figure 7. Numerous new peaks are observed after the dilution in triflic acid.

Figure 8 presents the infrared spectrum of a sample (17) that was dissolved in triflic acid for 48 h (11:CF_3SO_3H = 1:200), then precipitated in water (0.5 M in Na_2CO_3), and washed with water. Compared to the spectrum of the original sample, the carbonyl absorption at 1640 cm^{-1} and the absorption bands of monosubstituted phenyls (1073, 736, and 692 cm^{-1}) decrease after reaction with CF_3SO_3H. The bands at 843 and 768 cm^{-1} also decrease, and a new small band appears at 1033 cm^{-1}. Otherwise the spectrum is unchanged, revealing that most of the PEEK structure has been preserved in 17. The decrease in intensity of the monosubstituted phenyls vibration and of the carbonyl absorption supports reaction scheme R10. The new band at 1033 cm^{-1} may be due to the C–O stretching of 15.[35] This absorption corresponds to one of the absorption bands of triphenylcarbinol (1032 cm^{-1}).

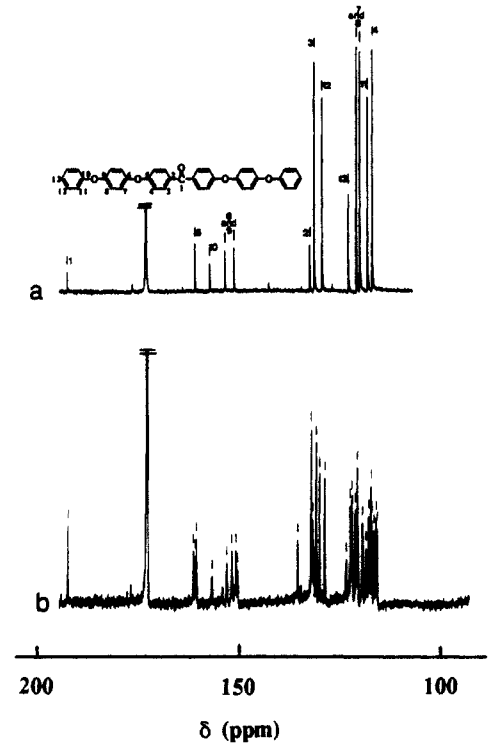

Figure 7. ^{13}C NMR spectra of EEKEE in *N*-methyl-2-pyrrolidone at 100 °C: (a) EEKEE without any treatment; (b) EEKEE after a 48-h dilution in triflic acid (CF_3SO_3H:EEKEE molar ratio = 250:1). The strong peak located at 173.3 ppm is due to the carbonyl group of the solvent. Chemical shift values for EEKEE in NMP are reported in Table III.

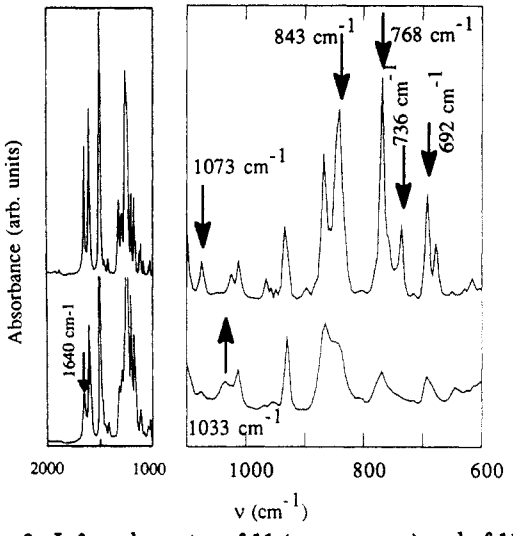

Figure 8. Infrared spectra of 11 (upper curve) and of 11 after 48 h in triflic acid (200:1) (lower curve).

The SEC chromatogram of 17 is compared to that of 11 in Figure 9. The chromatogram reveals the formation of di- and trimer from 11 during the 48-h reaction with triflic acid, providing a further confirmation for (R10).

We also attempted to follow (R10) by UV/visible spectroscopy. For tris(*p*-methoxyaryl)methylcarbenium ions λ_{max} occurs[36] at 483 nm, with ϵ_{max} = 50 000 L cm^{-1} mol^{-1}. For PEEK in methanesulfonic acid[37] λ_{max} = 413.8 nm and ϵ_{max} = 44 000 L cm^{-1} mol^{-1}. One may thus hope to observe the formation of 16 by UV spectroscopy. This is further supported by the fact that solutions turned slowly from deep orange to red-brown with reaction time. However, no significant changes were observed in the UV spectra. We speculate that this is due to the strong dilution

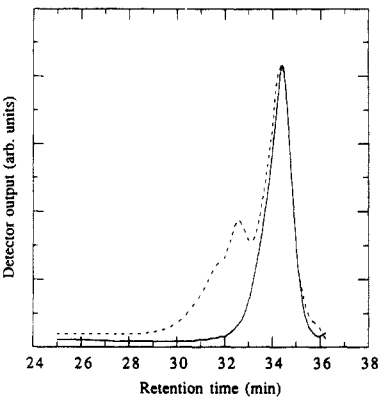

Figure 9. SEC chromatogram of 11 (continuous line) and of 11 after 48 h in triflic acid (200:1) (dashed curve).

of the reaction medium in triflic acid required before recording the UV spectra.

Reaction R10 is slow. For a 200:1 CF_3SO_3H:11 ratio, all the ketones have not reacted after 48 h, as shown in Figures 8 and 9. Moreover, (R10) is not able to compete significantly with acylations conducted at 70:1 CF_3SO_3H:11 dilution, as checked by the following experiment. Two acylations were performed using 10% excess of 4 at 70:1 CF_3SO_3H:11 dilution. In the first case, 11 was dissolved in triflic acid for more than 5 h before adding 4, while for the other case, 4 was added as soon as 11 was totally dissolved in triflic acid (~2 min). The final yields and the reaction kinetics were identical within 5%.

(b2) Side Reaction during the Acylation Reaction. Protonated ketones of fluoroaryl ketone chain ends are more electrophilic than protonated interior ketones. Thus, in addition to reaction scheme (R10–R11), another side reaction involving fluoroaryl ketone chain ends has to be considered in the acylation medium (R10′–R11′).

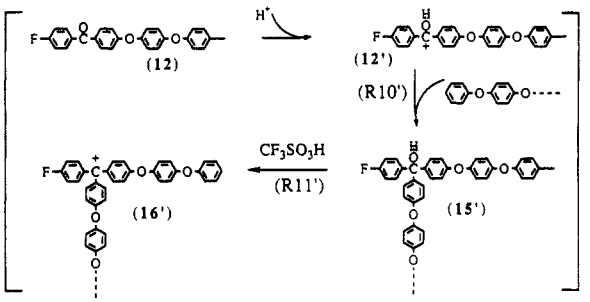

Initial acylations performed on the two longest phenoxy-ended oligomers in dilute conditions (~200:1) led to products having a bimodal molecular mass distribution, as observed by size exclusion chromatography (SEC). The second fraction eluted corresponds to the expected oligomer molecular mass, while the first fraction eluted is roughly double the expected molecular mass. Precise ^{19}F NMR of these mixtures confirmed the lack of fluorine, which was indicated by the small η obtained during the kinetic studies. The ^{13}C NMR spectra of these mixtures in CH_3SO_3H displayed some peak splittings and a few new peaks as compared to the expected products. The new peaks are listed in Table II, together with their tentative assignments based on structure 16 (16′ should have similar resonances). The carbenium resonance (carbon 1) is not observed probably because its concentration is at least one-third lower than the other carbons and is hidden in the background. The infrared spectra of the mixtures were typical of the desired products, except for the presence of a well-marked shoulder at 1028 cm^{-1}. The absorption peaks at 768 and 740–760 cm^{-1} were smaller

Table II
Estimated and Observed ^{13}C Chemical Shifts of the Triphenylmethylcarbenium Ion Produced by the (R10–10′) Side Reactions (Solvent: CH_3SO_3H)

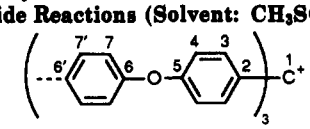

carbon	$\delta_{computed}$ (ppm)	δ_{obsd} (ppm)
1	210.9[a]	
2	136.2	134
3	128.4	130.3
4	119	123.3
5	156.4	163
6,6′	151.8[b]	150.6, 152.8
7,7′	123.6[b]	124.3, 123.0

[a] Chemical shift of triphenylmethanol measured in sulfuric acid solution.[38] [b] Chemical shift of similar carbons in the PEEK structure.

than expected. These observations indicate that (R10) or (R10′) indeed competes with the acylation. Since (R10) is relatively slow as compared to usual acylation kinetics, it is highly probable that (R10′) is the main side reaction competing with acylation.

The importance of the side reaction (R10′) relative to the desired acylation increases with increasing dilution, although the acylation rate also increases (Table I). This suggests that the side reaction is slower upon concentration of the reagents. We found indeed that for a 70:1 CF_3SO_3H:11 dilution, (R10′) is very slow. For instance, 11 was reacted with half the stoichiometric amount of 4 in triflic acid. Four hours after the end of the reaction, the other half equivalent of 4 was added. The final yield was identical to η obtained for reactions conducted without delaying the acylation.

However, (R10′) is rapid enough to compete with the acylation at higher dilutions. The reason for the acceleration of (R10′) upon dilution is not clear at the present time. It is unlikely that compounds as short as 11 could cyclize, although this is a serious possibility for the longer chain compounds. Perhaps some interference of the ionic shell around the protonated ketone could be invoked to explain the rate decrease of (R10′) upon concentration.

Conclusions. To produce the desired linear products, dissolution of the phenoxy-ended oligomers in triflic acid in the absence of acylating agent for long periods of time must be avoided because of (R10). Low dilutions, which considerably reduce the acylation rate, and high dilutions, which favor (R10′), should also be avoided. There is thus an optimal concentration range for the acylation. FK-(EEK)$_2$F is successfully produced from EEKEE using 10% excess of 4 and a 1:70 11:CF_3SO_3H dilution. Even if small amounts of side product are produced for such conditions (Table I), the subsequent recrystallization from NMP apparently eliminates this product.

However, recrystallization from NMP does not eliminate the side product from longer oligomers; hence, conditions which strongly favor the acylation must be found. Furthermore, longer oligomers are produced from longer phenoxy-ended compounds which possess more ketones whose protonation increases the amount of $CF_3SO_3^-$ in solution. This reduces the amount of the electrophilic acylating species in solution, following (R6) or (R7), and reduces the acylation rate. This rate can be increased by increasing the excess of 4 up to 300% for a 1:70 11:CF_3SO_3H dilution. As shown in Table I, the acylation rate constant decreases, but the overall reaction rate ($\tau_{1/2}^{-1}$) increases. These are the conditions selected for the final synthesis of FK(EEK)$_4$F from EEK(EEK)$_2$EE and of FK-(EEK)$_3$F from EEK(EEK)EE. Although the reactions

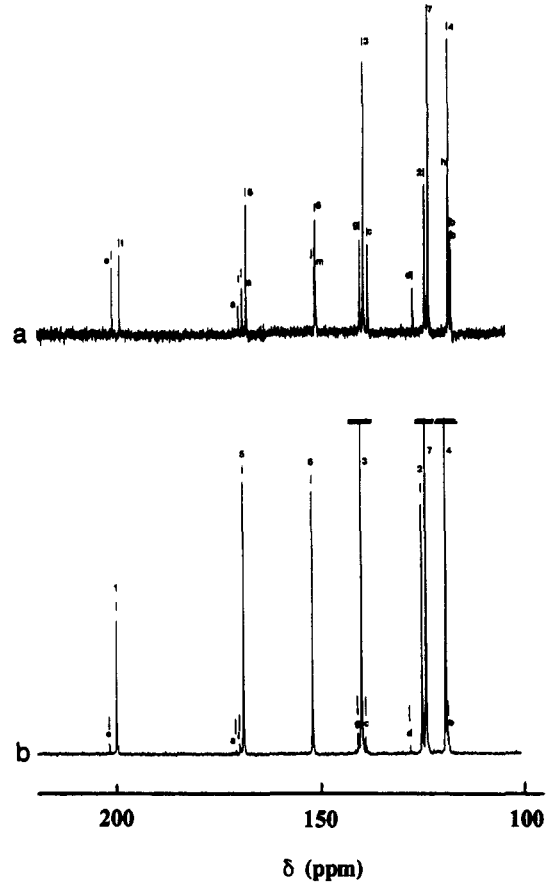

Figure 10. ^{13}C NMR spectra, taken in CH_3SO_3H, of (a) FK-(EEK)$_4$F and (b) fluoroaryl ketone-ended PEEK (polymer sample) (chemical shift values and carbon numbering are given in Table III).

are complete in less than 3 h, the products were precipitated only after 24 h. This is no problem since the fluoroaryl ketone-ended oligomers are stable in triflic acid for these concentrations.

^{13}C NMR Characterization. The proton-decoupled ^{13}C NMR spectra of the FK(EEK)$_n$F oligomers were recorded in CH_3SO_3H. A representative example is presented in Figure 10, together with the spectrum of a fully fluorine-terminated PEEK (M_n = ~ 9000). Assignments of the main peaks were based on previous assignments.[24] Chain end resonances were assigned using standard tables and by comparison of the oligomers and high polymer. The chemical shifts and the ^{13}C–^{19}F coupling constants (J_{CF}) are summarized in Table III.

Carbons e, g, and i have short-range environments identical to that of carbons 1, 3, and 5, respectively. However, these carbons are chemically inequivalent due to fluorine inductive effects transmitted via the π-electron framework. A weak fluorine influence can even be detected after the first ether bridge: the chemical shifts of carbons j and m are different from the chemical shift of carbon 6. This agrees with previous observations reported on PEEK.[39]

^{13}C NMR spectra of the phenoxy-ended oligomers could not be taken in CH_3SO_3H, because large amounts of these compounds—except EEKEE (Table III)—could not be dissolved in this acid. The solubilization of PEEK in strong acids is helped by ketone protonation. We believe that the phenoxy-ended oligomers dissolve only very slowly in methanesulfonic acid both because the oligomer chain packing is slightly different from the fluorine-ended oligomer chain packing[20] and because the first ketone is located deeper in the crystalline phase for the phenoxy-

Table III
^{13}C NMR Chemical Shifts of PEEK Oligomers

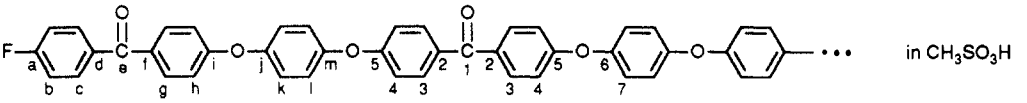

carbon	4,4'-difluoro-benzophenone	FK(EEK)$_1$F	FK(EEK)$_2$F	FK(EEK)$_3$F	FK(EEK)$_4$F	F-ended PEEK (polymer sample)
a	170.97, 168.86 (J_{CF} = 265 Hz)	170.90, 168.81 (J_{CF} = 263 Hz)	170.80, 168.81 (J_{CF} = 250 Hz)	171.0, 168.86 (J_{CF} = 269 Hz)	171.0, 168.80 (J_{CF} = 277 Hz)	171.0, —
b	118.10, 117.92 (J_{CF} = 23 Hz)	118.18, 118.04 (J_{CF} = 18 Hz)	118.19, 118.01 (J_{CF} = 23 Hz)	118.22, 118.04 (J_{CF} = 23 Hz)	118.16, 117.98 (J_{CF} = 23 Hz)	118.0
c	138.75	138.73	138.65, 138.56 (J_{CF} = 11 Hz)	138.76, 138.68 (J_{CF} = 10 Hz)	138.65, 138.57 (J_{CF} = 10 Hz)	138.5
d	128.37	127.42	127.2	127.42	127.48	127.5
e	204.32	202.07	202.15	202.06	202.05	202.0
1			200.2	200.18	200.19	200.13
f, 2		124.35, —	124.6, —	124.33, 124.47	124.49	124.4
g		140.74	140.59	140.88	140.63	140.8
3			139.69	139.74	139.66	139.57
h		118.71	118.82	118.78	118.77	
4			118.68	118.61	118.61	118.56
i		170.01	169.94	170.1	169.97	170.0
5			168.90	168.95	168.91	168.80
j, m		151.64	151.60, 151.92	151.53, 151.93	151.54, 151.92	
6				151.77	151.77	151.71
k, l, 7		123.75	123.61	123.64	123.56	123.44

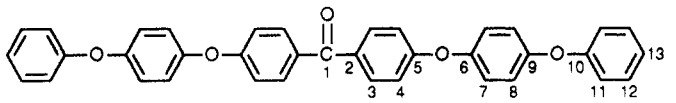

δ (ppm) in CH_3SO_3H
C_1, 199.5; C_2, 124.4; C_3, 139.6; C_4, 118.2; C_5, 169.3; C_6, 149.3; C_7, 122.9; C_8, 121.1; C_9, 155.4; C_{10}, 157.3; C_{11}, 119.3; C_{12}, 130.6; C_{13}, 124.0

δ (ppm) in NMP (100 °C)
C_1, 192.7; C_2, 132.6; C_3, 131.5; C_4, 117.0; C_5, 161.1; C_6/C_9, 151.1/153.7; C_7/C_8, 121.1/120.2; C_{10}, 157.5; C_{11}, 118.3; C_{12}, 129.6; C_{13}, 123.1

ended oligomers than for the F-ended oligomers. Therefore, diffusion of protons into the crystallites is more difficult in phenoxy-ended oligomers than in the F-ended ones. The solubilization of these oligomers is thus slower.

The ^{13}C spectrum of EEKEE agrees with the postulated structure. For other phenoxy-ended oligomers, other spectroscopic evidence (given below) suggests that the structures are also correct. However, the major fact which confirms the structure of these oligomers is that the F-ended oligomers produced from them by reaction R2 have been demonstrated by ^{13}C NMR to have the expected chemical structure.

Molecular Mass Characterization. A single elution peak was obtained by SEC for each compound. The linear relationship between the measured molecular mass and the expected theoretical mass is plotted in Figure 11. Although fluorine-ended oligomers FK(EEK)$_n$F have slightly lower molecular masses than phenoxy-ended oligomers EEK(EEK)$_{n-1}$EE, their SEC-measured molecular masses are larger. The hydrodynamic volume of F-ended oligomers is thus larger than that of the corresponding phenoxy-ended oligomers. This results from the fact that F-ended oligomers have one ketone bridge more than corresponding phenoxy-ended oligomers, and the ketone bridge is more rigid than the ether bridge due to electron delocalization with formation of a partial double bond at the ketone–phenyl bonds.

The molecular masses of fluorine-ended oligomers measured by ^{19}F NMR were equal to the expected theoretical values within the accuracy of the technique. No fluorine was detected in phenoxy-ended oligomers, confirming that the nucleophilic substitution was complete.

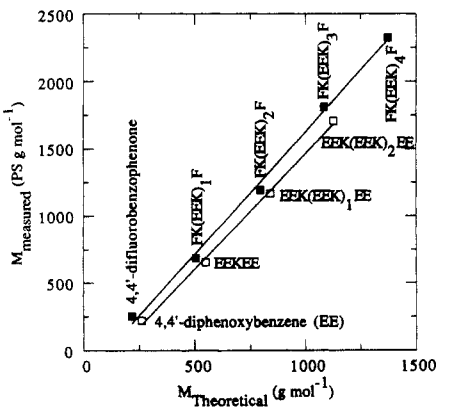

Figure 11. SEC-measured oligomer molecular masses (expressed in polystyrene (PS) equivalents) as a function of theoretical computed masses.

Infrared Spectroscopy. The infrared spectra of the oligomers are similar to the PEEK IR spectrum, except that peaks are broader for the polymer and that additional chain end peaks are observed in the oligomer spectra.

For phenoxy-ended oligomers, various peaks typical of monosubstituted phenyl rings are observed. The most characteristic bands are at 692 cm^{-1} (out-of-plane skeletal mode[35]), 730–750 cm^{-1} (out-of-plane CH bending,[35] broad shoulder), and 1073 cm^{-1} (CH in-plane deformation mode[35]). Figure 12 presents the ratio of the areas under the 1073-cm^{-1} absorption and the 1011-cm^{-1} peak (taken as reference, see ref 40) as a function of the reciprocal of the molecular mass. The linear relationship does not converge to zero probably because of some baseline choice problem.

For F-ended oligomers, none of the aforementioned peaks are observed. A shoulder located around 820–815

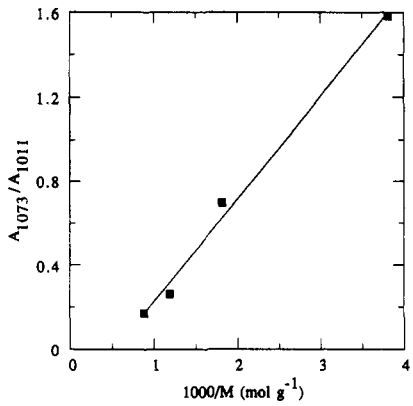

Figure 12. Evolution of the ratio of the 1073-cm^{-1} IR absorbance peak area (typical of monosubstituted phenyls) to a reference peak area (a phenyl vibration located at 1011 cm^{-1}) with the reciprocal of molecular mass M for phenoxy-ended oligomers.

cm^{-1} decreases in intensity with oligomer molecular mass, which must correspond to a C–F vibration. However, this peak is very weak and it is not possible to accurately determine its area. It is thus useless as a characterization tool for PEEK fluoroaryl ketone chain ends.

Experimental Section

Reagents. 4,4′-Difluorobenzophenone (7) was used as received from I.C.I. 4-Phenoxyphenol (2) (99%, Janssen) was recrystallized from petroleum ether before use. Sodium carbonate (pro analysis, Merck) was finely ground and dried overnight at 250 °C under vacuum before use. 4-Fluorobenzoic acid (4) (99%, Janssen) and trifluoromethanesulfonic acid (99%, Janssen) were used without further purification. 4,4′-Diphenoxybenzene was prepared by the Ullman route as described elsewhere[41] and then recrystallized in 2-propanol (calcd molecular mass, 262.099 g mol^{-1}, measured (FAB mass spectrometry), 262.1 g mol^{-1}; mp 75.8 °C (lit.[41] mp 76.5 °C)).

Solvents. Benzophenone (99%, Janssen) was used as received. N-Methyl-2-pyrrolidone (GAF) was distilled under vacuum and stored over molecular sieves. All other solvents (acetone, water, methanol) were distilled before use.

Nucleophilic Substitution. In a typical procedure, a three-necked flask was fit with a platinum thermometer, purge (dry argon) inlet, and a Dean–Stark trap, and 250 g of benzophenone (1.4 mol) was introduced, together with 1.5×10^{-2} mol of 2 (20% excess), 1.8×10^{-2} mol of sodium carbonate, and 30 mL of toluene. The flask was equipped with magnetic stirring and a heating mantel powered through a temperature controller. The temperature was raised to 140 °C and slowly (1–2 h) raised to 180 °C to allow phenolate formation and water/toluene azeotrope distillation. After most of the azeotrope was collected, the temperature was further increased to 250 °C and the last amounts of toluene were collected. FK(EEK)$_2$F (5 g, 6.3×10^{-3} mol) was then added, and the Dean–Stark trap was replaced by a simple air-cooled tube. The temperature was raised to 300 °C and held for 1.5 h. The heating power was then switched off, and the temperature was allowed to decrease to 200 °C. The hot liquid mixture was slowly poured into a large amount of distilled methanol, collected immediately on a sintered glass frit, and washed successively with methanol, acetone, and water. The powder was then refluxed successively in methanol and water. The product was hot filtered between each reflux and finally dried under vacuum at 120 °C. Recrystallization from N-methyl-2-pyrrolidone gave a white odorless powder (70–85% yield, depending on oligomer molecular mass).

Electrophilic Substitution. The reaction will be described for 8.6 g (1.56×10^{-2} mol) of EEKEE (11). Similar conditions are used for other oligomers, except with respect to the excess of 4, which varies between 10 and 300% (see the conclusions of the kinetic section). In an Erlenmeyer flask, 1.09 mol (~100 mL) of CF_3SO_3H was introduced, together with 3.44×10^{-2} mol of 4. Then 11 was slowly added, the Erlenmeyer was stoppered, and the mixture was stirred for 24 h. The solution was slowly poured into a large volume of 1.2 M aqueous Na_2CO_3 while continuously stirring. After filtration and washing with water, the product was refluxed in water, hot filtered, and washed again with water. The product was then refluxed in acetone, filtered, and washed with acetone. The product was dried under vacuum at 120 °C. Recrystallization from N-methyl-2-pyrrolidone gave a white odorless powder (70–80% yield, depending on the oligomer molecular mass).

^{19}F NMR. (1) Protonation Studies. Some protonation studies were conducted in sulfuric acid, scanning a large range of acid strengths. Between 30 and 50 mg of 4 or 7 was dissolved in 2 mL of sulfuric acid solution. The strength of the acid solution was varied either by adding increasing amounts of a weak base to concentrated sulfuric acid (99%+) or by adding increasing amounts of SO_3 to this acid. Acetone was selected as the weak base for solubility reasons. Because undiluted acetone condenses rapidly in concentrated H_2SO_4,[42] NMR measurements were performed within 1 h of the solvent preparation. CF_3SO_3Na was used as the internal standard. The spectra were recorded on a Bruker AM250, with a pulse width of 13 μs and a relaxation delay of 5.6 s.

Additional protonation studies were conducted in CF_3SO_3H to work in conditions similar to those of the synthesis reactions. In this case, increasing amouts of CF_3SO_3Na and FK(EEK)$_2$F or 4 were added. It was not possible to dissolve more than ~3 mg of CF_3SO_3Na in 1 mL of CF_3SO_3H. The spectra were recorded on a Bruker AM250, with a pulse width of 2 μs and a relaxation delay of 3 s. The chemical shifts were measured relative to the triflic acid resonance peak, which is actually a fast-exchange peak between CF_3SO_3H and $CF_3SO_3^-$; its location depends thus on the $[CF_3SO_3^-]/[CF_3SO_3H]$ ratio. However, we found that the location of the solvent peak is constant in the concentration range of the present study. This is easy to understand, since the $[CF_3SO_3^-]/[CF_3SO_3H]$ ratio was always lower than 10% and since the chemical shifts of $CF_3SO_3^-$ and CF_3SO_3H are expected to be similar.

(2) Kinetic Studies. A known amount of oligomer EEK(EEK)$_n$EE (usually n = 0) and a known amount of 4,4′-difluorodiphenyl sulfone (18) used as a quantitative standard were dissolved in 1 mL of CF_3SO_3H. A known amount of 4 was dissolved separately in 2 mL of CF_3SO_3H, and 1 mL was then added rapidly to the first solution at time zero. The reacting solution was vigorously shaken for 30 s, and a sample was introduced into a standard ^{19}F NMR tube. The acquisition began immediately on a Bruker AM250 with the following settings: scan frequency, 235.35 MHz; pulse width, 0.8 μs; relaxation delay, 3 s; number of scans, 150. A low value of pulse width was selected to allow a fast return to equilibrium to reduce the total acquisition time. Each accumulation took ~8 min. Successive accumulations were taken until no more evolution was detectable. A final accumulation was taken ~12 h later to ensure that the reaction was really complete. The evolution of the reaction was measured by computing the areas under the resonance peak of each substance. The initial amount of EEK(EEK)$_n$EE in the NMR tube was known since its ratio to 18 was a known quantity. The chemical shifts of each substance were computed using the solvent peak as reference.

(3) Molecular Mass Determinations. ^{19}F NMR was also used to determine the number-average molecular mass of the fluorine-ended oligomers as described previously,[39] except that 18 was used as the quantitative standard instead of CF_3COOH.

^{13}C NMR. Spectra were recorded in methanesulfonic acid on a Bruker AM500, operated in the broad-band mode. Experimental settings were as follows: concentration, ~37 mg mL^{-1}; pulse width, 15 μs; relaxation delay, 3 s; scan frequency, 125.76 MHz. The solutions were filtered through a 1-μm Teflon filter before measurements. Tetramethylsilane was used as internal standard.

Infrared Spectroscopy. The IR spectra were recorded in a Perkin-Elmer 580B dispersive spectrometer, using KBr pellets and an instrument resolution of 2.3 cm^{-1}.

Assessment of Side Reaction by UV Spectroscopy. 11 was dissolved in triflic acid ($n_{(CF_3SO_3H)}:n_{(11)}$ = 200:1), and small aliquots of the solution were regularly taken and strongly diluted

in triflic acid. The UV spectra of the diluted solutions were then recorded with a Gilson UV/vis spectrophotometer from 250 to 750 nm.

Size exclusion chromatography was performed at 115 °C with a 50/50 (w/w) phenol/trichlorobenzene eluant using a Waters 150C chromatograph equipped with two Shodex mixed-bed columns, one Ultrastyragel (500 Å) column, and a refractive index detector. Four-milligram samples were dissolved in 2 mL of solvent by holding and shaking the solution at 160 °C for 30 min. The results were analyzed on a Digital microVax 2000. The chromatograph was calibrated with 13 polystyrene standards ranging from 580 to 2 700 000 g mol^{-1}. The molecular mass corresponding to the maximum of the retention peak was computed for each oligomer and expressed in polystyrene equivalents (PS g mol^{-1}).

Acknowledgment. We are indebted to Dr. H. M. Colquhoun for his helpful comments. Prof. J.-M. and Mrs. C. Dereppe are kindly acknowledged for their help with the NMR technique as are C. Fagoo and D. Daoust for the SEC technique and M.-F. Sallets for the UV/vis facilities. Part of the experimental work of this study was performed by K. Lemaire during a student work. Special thanks are due to Y. Charlier, who acquainted A.J. with chemistry techniques, and to Drs. J. Marchand and J. Penelle for their careful reading of the manuscript. We also acknowledge the referees for their pertinent suggestions.

References and Notes

(1) Research Assistant of the Belgian National Fund for Scientific Research.
(2) Dawson, P. C.; Blundell, D. J. *Polymer* **1980**, *21*, 577.
(3) Rueda, D. R.; Ania, F.; Richardson, A.; Ward, I. M.; Balta Calleja, F. J. *Polym. Commun.* **1983**, *24*, 258.
(4) Hay, J. N.; Kemmish, D. J.; Langford, J. I.; Rae, A. I. M. *Polym. Commun.* **1984**, *25*, 175.
(5) Wakelyn, N. T. *Polym. Commun.* **1984**, *25*, 306.
(6) Fratini, A. V.; Cross, E. M., Whitaker, R. B.; Adams, W. W. *Polymer* **1986**, *27*, 861.
(7) Harris, J. E.; Robeson, L. M. *J. Polym. Sci., B: Polym. Phys.* **1987**, *25*, 311.
(8) Abraham, R. J.; Haworth, I. S. *Polymer* **1991**, *32*, 121.
(9) Wakelyn, N. T. *J. Polym. Sci., C: Polym. Lett.* **1987**, *25*, 25.
(10) Hay, J. N.; Langford, J. I.; Lloyd, J. R. *Polymer* **1989**, *30*, 489.
(11) Blundell, D. J.; Osborn, B. N. *Polymer* **1983**, *24*, 953.
(12) Lee, Y.; Porter, R. S. *Macromolecules* **1988**, *21*, 2770.
(13) Cheng, S. Z. D.; Cao, M.-Y.; Wunderlich, B. *Macromolecules* **1986**, *19*, 1868.
(14) Jonas, A.; Legras, R. In *Advanced Thermoplastics and Their Composites*; Kausch, H. H., Ed., in press.
(15) Lovinger, A. J.; Davis, D. D. *Polym. Commun.* **1985**, *26*, 322.
(16) Lovinger, A. J.; Davis, D. D. *Macromolecules* **1986**, *19*, 1861.
(17) Waddon, A. J.; Hill, M. J.; Keller, A.; Blundell, D. J. *J. Mater. Sci.* **1987**, *22*, 1773.
(18) Tsuji, M.; Kawamura, H.; Kawaguchi, A.; Katayama, K. *Bull. Inst. Chem. Res., Kyoto Univ.* **1989**, *67*, 77.
(19) Legras, R.; Leblanc, D.; Daoust, D.; Devaux, J.; Nield, E. *Polymer* **1990**, *31*, 1429.
(20) Jonas, A.; Legras, R.; Scherrenberg, R.; Reynaers, H. second paper of this series, to be published.
(21) Jonas, A.; Legras, R. third paper of this series, to be published.
(22) Attwood, T. E.; Dawson, P. C.; Freeman, J. L.; Hoy, L. R. J.; Rose, J. B.; Staniland, P. A. *Polymer* **1981**, *22*, 1096.
(23) Roberts, R. M. G.; Sadri, A. R. *Tetrahedron* **1983**, *39*, 137.
(24) Colquhoun, H. M.; Lewis, D. F. *Polymer* **1988**, *29*, 1902.
(25) Deno, N. C.; Pittman, C. U.; Wisotsky, M. J. *J. Am. Chem. Soc.* **1964**, *86*, 4370.
(26) Olah, G. A.; Schleyer, P. v. R., Eds. *Carbonium Ions*; Wiley-Interscience: New York, 1976; Vol. 5.
(27) Olah, G. A.; Iyer, P. S.; Surya Prakash, G. K.; Krishnamurthy, V. V. *J. Org. Chem.* **1984**, *49*, 4317.
(28) Olah, G. A.; Iyer, P. S.; Surya Prakash, G. K.; Krishnamurthy, V. V. *J. Am. Chem. Soc.* **1984**, *106*, 7073.
(29) Gillespie, R. J.; Peel, T. E. *Superacid Systems.* In *Advances in Physical Organic Chemistry*; Gold, V., Ed.; Academic Press: London, 1971; Vol. 9.
(30) Olah, G. A.; Surya Prakash, G. K.; Sommer, J. *Superacids*; John Wiley and Sons: New York, 1985.
(31) Howells, R. D.; McCown, J. D. *Chem. Rev.* **1977**, *77*, 69.
(32) Wehrli, F. W.; Marchand, A. P.; Wehrli, S. *Interpretation of Carbon-13 NMR Spectra*, 2nd ed.; John Wiley and Sons: Chichester, 1988.
(33) It is important to realize that this does not imply that the ratio $n_{(4)}/n_{(8)}$ of unprotonated to protonated fluorobenzoic acid is constant during the experiments, since small variations in the $n_{(8)}/(n_{(4)} + n_{(8)})$ ratio correspond to much larger variations of $n_{(4)}/n_{(8)}$ when this ratio is small as it is in our experiments.
(34) March, J. *Advanced Organic Chemistry: Reactions, Mechanisms, and Structure*, 3rd ed.; John Wiley and Sons: New York, 1985.
(35) Bellamy, L. J. *The Infrared Spectra of Complex Molecules*, 3rd ed.; Chapman and Hall: London, 1975; Vol. 1.
(36) Olah, G. A.; Schleyer, P.v.R., Eds. *Carbonium Ions*; Wiley-Interscience: New York, 1968; Vol. 1.
(37) Daoust, D.; Devaux, J.; Godard, P.; Jonas, A.; Legras, R. In *Advanced Thermoplastics and Their Composites*, Kausch, H. H., Ed., in press.
(38) Olah, G. A.; Baker, E. B; Comisarow, M. B. *J. Am. Chem. Soc.* **1964**, *86*, 1265.
(39) Devaux, J.; Daoust, D.; Legras, R.; Dereppe, J. M.; Nield, E. *Polymer* **1989**, *30*, 161.
(40) Jonas, A.; Legras, R.; Issi, J.-P. *Polymer* **1991**, *32*, 3365.
(41) Neville, R. G.; Mahoney, J. W. *J. Appl. Polym. Sci.* **1967**, *11*, 2029.
(42) Liler, M. *Reaction Mechanisms in Sulphuric Acid*; Academic Press: London, 1971.